Mechanisms of Electrotunable Friction in Friction Force Microscopy Experiments with Ionic Liquids

Karina Pivnic[1], Oscar Y. Fajardo[1,2], Fernando Bresme[2], Alexei A. Kornyshev[2], and Michael Urbakh[1*]*

[1]School of Chemistry, and The Sackler Center for Computational Molecular and Materials Science, Tel Aviv University, Tel Aviv 6997801, Israel

[2]Deparment of Chemistry, Imperial College London, SW7 2AZ London, U.K.

Abstract

Using molecular dynamics simulations and a coarse-grained model of ionic liquids, we study mechanisms of electrotunable friction measured in friction force microscopy experiments, where only one layer of ionic liquid (IL) is present between the tip and electrode (substrate). We show that the variation of the friction force with the electrode surface charge density is determined by the regime of motion of the confined IL relative to the substrate and tip. The latter depends on the strengths of the ion-substrate and ion-tip interactions and on the commensurability between the characteristic ion dimensions and lattice spacings of the substrate and tip surfaces. Related with those factors, our simulations predict two strictly different scenarios for the variation of the friction force with the electrode surface charge. Revealing mechanisms of frictional energy dissipation in nanoscale IL films offers a way for controlling friction by tuning ion-substrate interactions and electrical polarization of sliding surfaces.

Introduction.

Tribology, the science of friction, wear, and lubrication, is of fundamental importance in many branches of pure and applied science.[1,2] The study of the nanoscale aspects of lubrication is attracting particular attention, as under normal loads, the active lubricant is just a few molecular layers thick. Friction mediated by nanoscale films is determined by the properties of these films under ultra-high confinement conditions, and depends crucially on the interactions with the confining solid surfaces. The future of nanotribology lies in new ways to switch and control surface interactions, reversibly and non-invasively, at the molecular level, and thereby tune friction. The ability to control and manipulate adhesion and friction during sliding[3,4,5,6,7] is extremely important for a large variety of applications in automotive and electronics industries, and even in medicine.

A unique path to controlling and ultimately manipulating lubricating properties of nanoscale fluid films confined between solid surfaces is through a polarization of sliding surfaces. By varying the electric potential, the composition and structure of the lubricating film may be dramatically changed, and the solid surfaces can quickly and reversibly be decorated with adsorbed (sub)monolayer or multilayers. This can be achieved in friction experiments performed under electrochemical conditions, using electrolyte solutions as lubricants. In such systems, when the surfaces are conductive, their potentials can be independently varied relative to a reference electrode in the bulk, as it was done in friction force microscopy (FFM) measurements.[8,9,10,11] Experiments on electrotunable friction with surface force apparatus (SFA) are on the way.[7,12,13]

Room **T**emperature **I**onic **L**iquids (RTILs) have recently attracted considerable interest as lubricants due to their unique physical properties, in particular low vapor pressure, wide electrochemical stability window and the virtually unlimited variety of

RTILs and their mixtures.[14,15,16,17] The interaction of RTILs with confining surfaces induces fascinating structural and dynamical features; to list some: layering, overscreening and crowding,[16,18] a discrete multi-valued friction behavior as a function of the load and the number of the confined ionic layers ("quantized friction"),[19] nanoscale capillary freezing of RTILs confined between metallic surfaces,[20] as well as electrotunable friction.[10,11] The latter represents one of the most promising properties of RTILs as lubricants, since for a given lubricant and under given tribological conditions (normal load, pulling velocity and temperature) the friction can be reversibly tuned via application of an electric field. So far, electrical control of nanoscale friction has been demonstrated only with the FFM experiments,[10,11] which due to the limited resolution allows mainly measurements with monolayer films confined between the tip and the substrate. In particular, FFM experiments in RTILs confined between the silica tip and graphite electrode[11] demonstrated that super-low friction (superlubricity) can be ‘‘switched’’ on and off in situ, by polarizing its surface relative to the reference electrode.

Friction phenomena in RTILs have also been studied through computer simulations performed at various levels of system idealization.[21,22,23,24,25,26,27,28,29,30] These works demonstrated that the shape of RTIL molecules may affect their layering structure, and pointed out the strong influence of in-plane ordering on friction. Recently, we reported the first simulations of electrotunable lubricity in RTILs[24,27,29,30] that revealed dramatic changes in the structure of the lubricating film upon charging the surfaces, and suggested possible scenarios for the electrical control of friction. However, despite the fact that up to now, experimental studies of the effect of the applied electric field on nanoscale friction have been performed only with the use of FFM, all simulations have been carried out for the configuration mimicking SFA, where

multilayered RTIL films are confined between flat surfaces. Unlike the SFA, the FFM experiments feature a lower level of confinement and different regimes of shear induced motion of ionic liquid (IL). Hence, establishing how these conditions affect the friction force is a necessary step to advance in a consistent interpretation of friction forces measured using different experimental techniques, as well as computer simulations.

In this paper, we investigated mechanisms of electrotunable friction studied in FFM experiments with RTILs using a coarse-grained description of the liquid. We found that the variation of the friction force with the electrode surface charge density is strongly affected by the regime of motion of the confined ionic liquids (ILs) relative to the substrate and the tip. The latter depends on the strengths of the ion-substrate and ion-tip interactions and on the commensurability between the characteristic ion dimensions and lattice spacings of the substrate and tip surfaces. Related with those factors, our simulations predict two strictly different regimes for the variation of the friction force with the electrode surface charge.

Model.

We perform non-equilibrium molecular dynamics simulations using the set up shown in Figures 1a,b. Here in accordance with experimental conditions, the region confined between the substrate and the FFM tip is in contact with a reservoir fluid. Hence, the chemical potential in the confined region is determined by the chemical potential of the reservoir by allowing the IL to enter or leave that region in response to shear and to changes in the normal pressure, temperature, or surface charge.

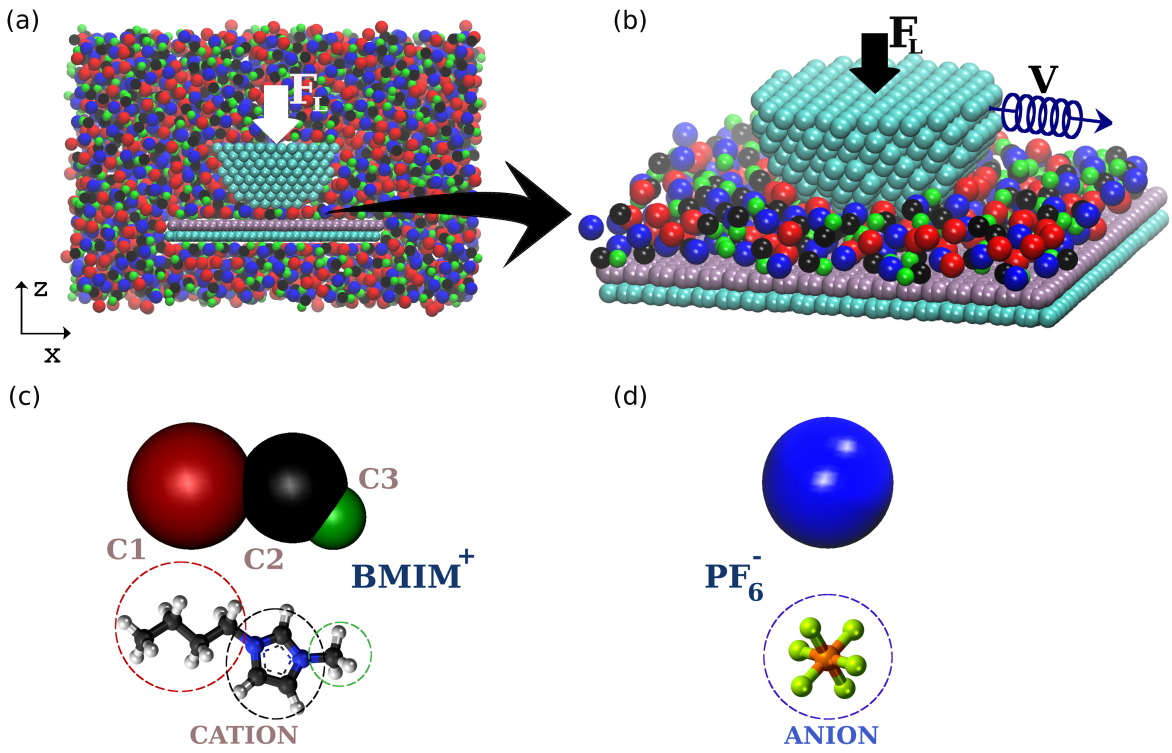


Figure 1. (a) Sketch of the FFM set-up with graphite substrate and silica tip in a typical fully periodic simulation containing the ionic liquid. (b) Snapshot showing the interfacial ionic liquid layer the tip reaches under a normal load, F_L, acting on the tip, which moves along the y axis at constant velocity V. The charged atomic layer of the substrate used for the electrotunable friction is highlighted in a gray color. The ionic liquid consists of $BMIM^+$ (c) cations and PF_6^- (d) anions modeled using a coarse-grained force field.[31] The following charges, $q_{C1} = 0.1848e, q_{C2} = 0.4374e, q_{C3} = 0.1578e, q_{anion} = -0.78e$ were assigned to the beads, C1, C2, C3 of the cation, and to the anion, respectively.

For the ionic liquid we consider 1-butyl-3-methylimidazolium hexafluoro phosphate, [BMIM][PF_6], using the coarse-grained force field proposed in reference (*31*), which provides a good description of static and dynamic properties, specifically viscosity and diffusion coefficients. Here, the PF_6^- anion is represented by a single negatively charged sphere, whereas the cation is modeled by three charged overlapping spheres, which represent the anisotropic charge and size distributions of the cation (see Figures 1c,d). This model for the ionic liquid has been recently used for simulations of

friction in surface force apparatus setup[27,29] where the ionic liquid was confined between mica plates. In this paper, focusing on FFM experiments, we consider the widely used graphite substrate and silica tip.[10,11,32,33] In the simulations, the graphite substrate is modelled as two AB-stacked layers of graphene. Although silica tips used in experiments are usually amorphous, in the simulations we limit ourselves to a simplified model considering a semispherical crystalline tip with FCC {111} surface lattice, which emulates the hexagonal patterns of the SiO_4 units of silica crystal structure. The radius of the tip is chosen to be 2nm.

The electrostatic potential of the substrate, which is controlled in experiments by applying a potential bias between the substrate and a reference electrode, was set up by assigning partial charges to the surface atoms in contact with the confined liquid. The substrate surface charge density, q_s, was varied between -32 and +32 μC/cm^2. This is the typical interval of the substrate charge density explored in the FFM experiments with ILs.[10,11] As for the tip, most of the simulations presented in the text have been done for an uncharged tip. Nevertheless, some experiments and simulations indicated that silica tip can be slightly negatively charged in ILs.[34,35] Therefore, we have also performed simulations for the tip surface charge density of -16 μC/cm^2. The results of these simulations have shown similar trends of the dependence of friction on substrate surface charge density as the results of simulations for an uncharged tip (see Supporting Information (SI)).

In addition to the Coulombic interactions, the beads representing ions interacted with other beads or atoms of the tip and the substrate through short range Lennard-Jones interactions (see the *Computational Methods* section for relevant parameters). The results of the simulations presented below were performed using an ionic-liquid/tip interaction, $\varepsilon_{it} = 1.25$ kJ/mol (the same for both cations and anions), which results in

a partial wetting of uncharged silica with a contact angle of $\sim 30^0$.[25] As for the ionic-liquid/substrate interaction, we explored a wide range of strengths, ε_{is}, ranging from 0.23 to 70 kJ/mol. Here the lowest value, $\varepsilon_{is} = 0.23$ kJ/mol, was obtained by the Lorentz-Berthelot combining rules from the IL-IL and graphite-graphite interactions.[36] The Lorentz-Berthelot combining rules are commonly employed when no fitted cross-interaction parameters are available. However, it should be noted that the height of potential barriers opposing the ion sliding along the surface, which is the key factor controlling interfacial friction, depends both on the strength of the ion-solid interaction and on the ratio between the surface periodicity and the characteristic dimensions of the ion (see Figure 2 and discussion there). The use of the coarse-grained description of the IL, taken here, where the cations and anions are represented by few large beads, smears the molecular structure of ions and may lead to a significant underestimation of the corrugation of the sliding potential energy landscape. This effect is more pronounced at the IL-graphite interface than at the IL-silica interface, since the periodicity of graphite lattice is smaller than that of silica. In order to compensate this possible drawback and to examine the effect of the corrugation of the sliding potential energy profile on friction we performed simulations in a broad range of strengths of ion-substrate interactions. As we show below, the strength of ion-substrate interaction controls the regime of motion of confined ions that in turn determines the charge dependence of friction.

The friction process was simulated by pulling the tip through a spring of stiffness, K=5 N/m, at a constant velocity, typically V=1 m/s, while the substrate was kept in the original position by using a restraining harmonic potential applied to all atoms. In accordance with FFM experiments,[10,11] where, due to the limited resolution, the frictional forces were measured when only one ionic liquid layer was present

between the surfaces, we also considered such a configuration applying a required normal force to the tip. The heating produced during the sliding motion was removed by using thermostats in the substrate and tip surfaces (see the Method section for simulation details). The simulation set up discussed above leads to erratic stick-slip motion compatible with experimental measurements of friction.

Computational Methods.

Non-equilibrium Molecular dynamics simulations of friction were performed using Grand Canonical Molecular Dynamics (GCMD) simulations.[37,38,39] In this method, the region between the tip and the substrate is simulated explicitly by setting the tip and the substrate in the bulk fluid (see Figure 1). This region is in contact with a reservoir fluid, hence the chemical potential in the region is determined by the chemical potential of the reservoir by allowing the ionic liquid to enter or leave it as a response to changes in the normal pressure, temperature or surface charge.[39] The electroneutrallity of the simulated system was preserved for all values of surface charge densities.

The confining “graphite” electrode and "silica" tip employed here are flexible. The electrode includes two graphene layers in the optimal stacking configuration. Each layer consists of 2052 atoms. The atoms in a layer are arranged in a honeycomb lattice with the lattice parameter of 0.24 nm, and the interlayer distance is set to 0.335 nm. The atoms interact through a Lennard-Jones potential with the interaction strength of 5 kJ/mol. The effective Lennard-Jones diameter of the atoms located in the same layer was set to 0.12 nm, while for the atoms located in different layers the Lennard-Jones diameter was set to 0.337 nm.

A hemispherical tip of radius 2 nm was cut from the FCC atomistic block with the lattice spacing of 0.36 nm. The tip consists of 548 atoms. The atoms in the tip

interact through a strong Lennard-Jones potential with the interaction strength of 50 kJ/mol, and the effective Lennard-Jones diameter of the atoms was set to 0.3218 nm. The strength of the Lennard-Jones potential describing interaction between atoms in the tip and substrate was set to 0.48 kJ/mol. The tip and substrate were arranged in the simulation box on the *xy* plane (see Figure 1). It should be noted that a complex geometrical structure and chemical reactivity of the tip used in FFM experiments may influence heights of potential barriers associated with the motion of ions.[40] These effects will be tested through the fully atomistic simulations which are planned in our further research.

Our simulations involved typically 1800 cation and anion pairs that were added to the simulation box containing the tip and substrate (see Figure 1). Depending on surface charge the number of cations and anions in the simulations box was slightly changed to preserve overall electroneutrality. In addition to the Coulombic interactions, the beads composing cations and anions interact with other beads or atoms in the tip and the substrate according to short range Lennard-Jones interactions with the parameters:[31] $(\sigma, \varepsilon)_{C1}$= (0.504 nm, 1.83 kJ/mol), $(\sigma, \varepsilon)_{C2}$=(0.438 nm, 2.56 kJ/mol) and $(\sigma, \varepsilon)_{C3}$= (0.341 nm, 0.36 kJ/mol) and $(\sigma, \varepsilon)_{anion}$= (0.506 nm, 4.71 kJ/mol) for the anions. The following charges, $q_{C1} = 0.1848e, q_{C2} = 0.4374e, q_{C3} = 0.1578e, q_{anion} = -0.78e$ were assigned to the beads, C1, C2, C3 of the cation, and to the anion, respectively. Further we used $(\sigma, \varepsilon)_{it}$= (0.3218 nm, 1.25 kJ/mol) for the ion-tip interactions and $(\sigma, \varepsilon)_{is}$= (0.337 nm, 0.23 kJ/mol) or $(\sigma, \varepsilon)_{is}$= (0.337 nm, 70 kJ/mol) for the ion-substrate interactions. The cross interactions between sites of type *i* and *j* were derived from these parameters using standard combining rules, *i.e.*, σ_{ij}= $(\sigma_i + \sigma_j)/2$ and $\varepsilon_{ij} = \sqrt{\varepsilon_i \varepsilon_j}$.

In order to achieve well-equilibrated configurations with one ionic layer

between the tip and the substrate, we first performed simulations with the applied normal pressures of 210 MPa for $\varepsilon_{is} = 0.23$ kJ/mol and 1.4 GPa for $\varepsilon_{is} = 70$ kJ/mol but no shear. These simulations involved about ~14 ns. After this pre-equilibration, the system was subjected to shear for about 28 ns, by pulling the tip through a spring at a constant velocity, as discussed in the text. Shearing heats the entire system. To prevent this, we coupled the tip and substrate atoms to a thermostat (using the v-rescale method[41]) at 450 K, while the ions were not coupled to an explicit thermostat. For all values of surface charge density and normal loads considered in this work, our simulations exhibit a stick-slip regime of friction. In this regime the frictional energy dissipation is determined by the heights of potential barriers at the solid-liquid interfaces, and the actual mechanisms of coupling to a thermostat makes only a small contribution to the overall energy dissipation.[2] All the simulations were performed by coupling the entire system to an anisotropic Berendsen barostat set at 1 bar pressure, which was applied in the *x* and *z* directions, keeping constant the box length in the direction of pulling, *y*. Periodic boundary conditions were imposed in all directions.

The equations of motion were integrated with the Leap-Frog algorithm and a time step of 2 fs, using the code Gromacs v. 4.6.3.[42] The long range electrostatic interactions were computed using the 3D –Particle Mesh Ewald summation method using "tin-foil" boundary conditions. Configurations were stored every 6 ps for further structural and dynamics analyses.

Results and Discussion.

The friction forces are determined by the potential energy landscape experienced by the ions sliding along the surfaces. In Figure 2 we present the two-dimensional potential energy surfaces for the C2 cation bead sliding in x, y-directions along the graphite

(Figure 2a) and silica (Figure 2b) surfaces, respectively. The corresponding cross-sections of potential energy surfaces in the sliding y-direction are shown in Figures 2c,d. The potential energy surfaces calculated for other beads representing the cations and anions show similar behavior. The corrugation of the sliding potential energy surfaces depends on both the strength of the ion-solid interaction and on the ratio between the surface periodicity and the characteristic dimensions of the ion (bead radii). The periodicity of the graphite surface, 0.24nm, is smaller than the bead diameter, $\sigma_{C2} = 0.4380$ nm, whereas the periodicity of the model silica surface, 0.36nm,[27] is similar to σ_{C2}, and therefore the sliding energy landscape on graphite is significantly smoother than that for silica. For low strength of the ionic/graphite interaction ($\varepsilon_{is} = 0.23$ kJ/mol) the heights of the potential energy barriers are smaller than k_BT (blue line in Figure 2c), and the ions can slide "smoothly" along the graphite surface. In contrast, the barriers for sliding along the silica surface are considerably higher than k_BT, and the ions are trapped in the potential minima (see Figure 2d). Only for strong enough ion/graphite interaction ($\varepsilon_{is} = 70$ kJ/mol) the sliding potential energy barriers at the graphite surface become comparable to those for the silica surface (red line in Figure 2c). The charging of the graphite electrode brings the counter-ions closer to the surface, and the corrugation of the sliding potential energy surfaces increases.

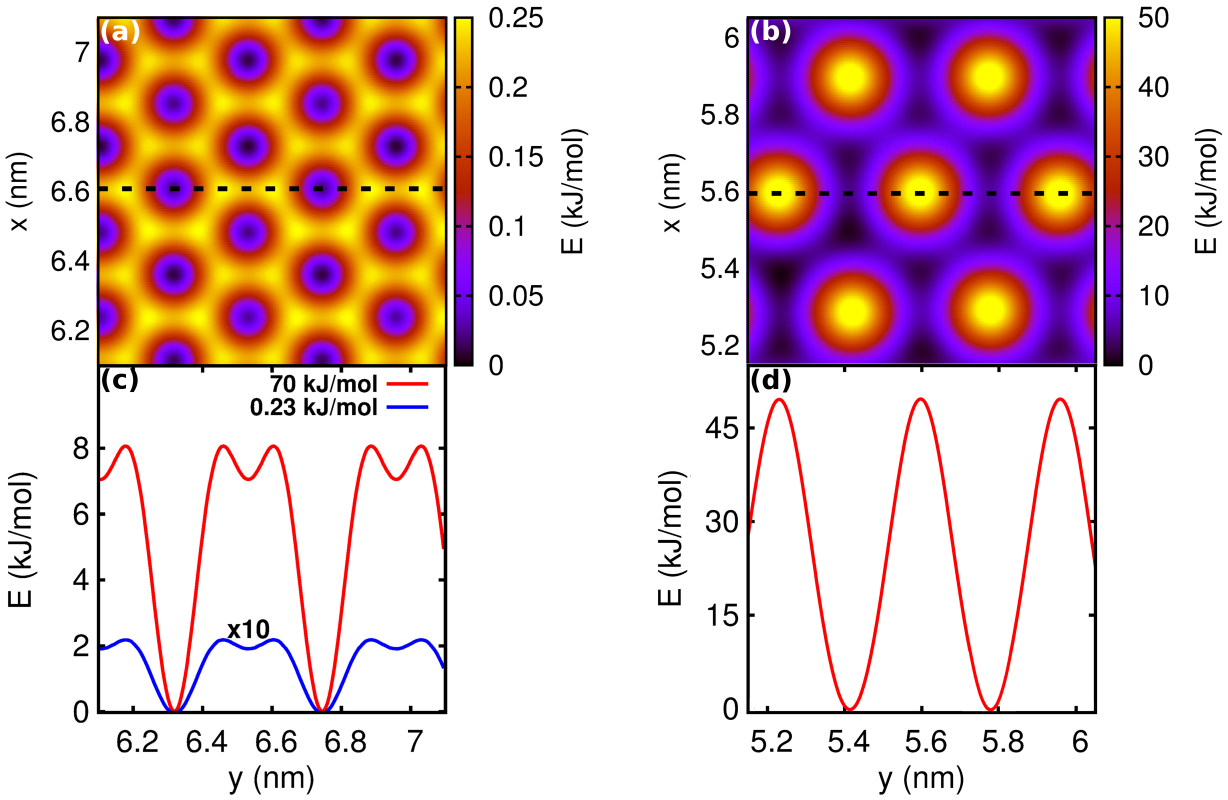


Figure 2. Two dimensional potential energy surface for the C2 cation bead sliding in x,y-directions along the (a) uncharged graphite surface with ion-substrate interaction $\varepsilon_{is} = 0.23$ kJ/mol, and along the (b) uncharged silica tip surface with ion-tip interaction $\varepsilon_{it} = 1.25$ kJ/mol. The black dashed lines in top panels correspond to the cross-sections of potential energy surfaces in the sliding y-direction, at a fixed x value. The potential energy profiles calculated along these lines at graphite and silica surfaces are shown in panels (c) and (d), respectively. In (c) blue and red curves describe the cases of weak and strong ion-substrate interactions, $\varepsilon_{is} = 0.23$ and 70 kJ/mol, respectively. For clarity, the blue line is scaled by a factor of 10. The calculations presented in panel (d) are done for $\varepsilon_{it} = 1.25$ kJ/mol.

In Figure 3, we report the time-averaged number densities of different charged groups of the ionic liquid layer across the confined region. The presented results have been calculated during sliding with velocity of 1 m/s, however they are only slightly different from the number densities in equilibrium. The information on the number densities of charged groups is essential for understanding the electrovariable friction mechanism. The top and bottom panels show results obtained for weak and strong ion-substrate

interactions, $\varepsilon_{is} = 0.23$ kJ/mol and $\varepsilon_{is} = 70$ kJ/mol, and the first, second and third columns correspond to the substrate surface charge densities of -32, 0, and +32 μC/cm^2, respectively. The presented densities are calculated for the uncharged tip, while the results for the negatively charged tip are presented in SI. In each of these panels, the vertical left and right dashed lines show the position of surface layers of substrate atoms and the tip apex, respectively.

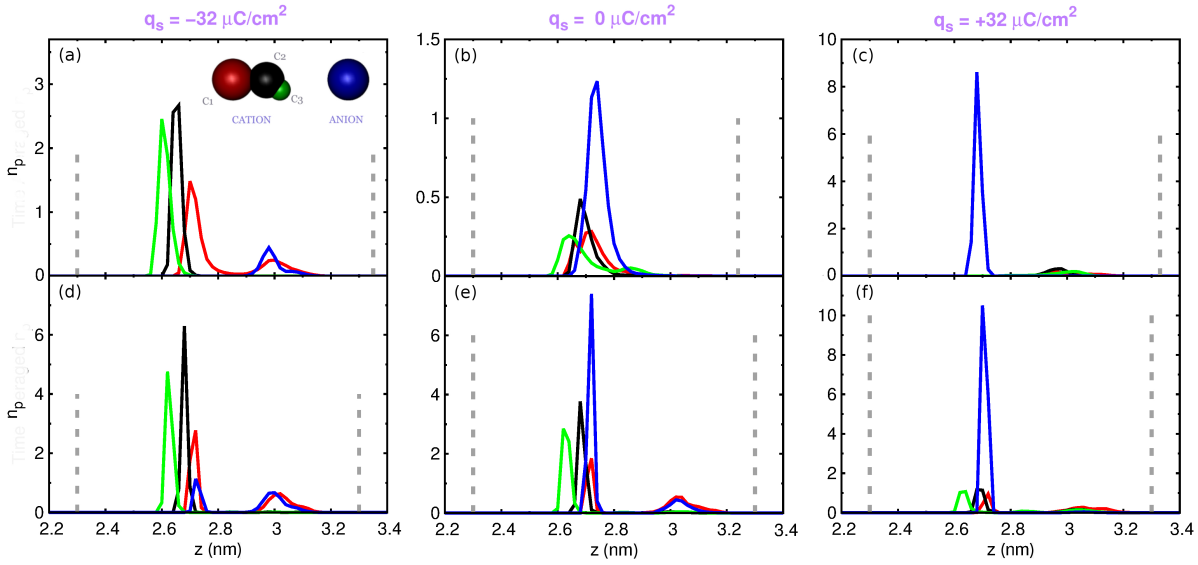


Figure 3. Number density of beads, n_p, corresponding to different charged groups across the region confined between the tip and the substrate. Results in panels (a-c) calculated for a weak ion-substrate interaction $\varepsilon_{is} = 0.23$ kJ/mol, whereas the results in (d-f) found for strong ion-substrate interaction $\varepsilon_{is} = 70$ kJ/mol. The first, second, and third columns correspond to the substrate surface charge densities of -32, 0, and +32 μC/cm^2, respectively. In each of these panels, the vertical left and right dashed lines show the position of surface layers of substrate atoms and the tip apex, respectively.

The composition of the interfacial IL layer exhibits similar dependence on the surface charge density for both values of the strength of ion-substrate interaction. For negative and positive surface charge densities, the IL layer consists mainly of cations and anions, respectively, whereas the layer on the uncharged surface includes a mixture

of cations and anions. The cations adsorbed at a negatively charged and uncharged graphite surface show two preferential orientations, one of them is "flat" and the other one "tilted", with the largest site (C1) pointing to the tip (see Figure 4a). The orientation of adsorbed cations can be characterized by the angle, θ, between the cation C1-C2 axis and the surface normal, as shown in Figure 4a.

With increase in the ion-substrate interaction, more ions would benefit energetically from adhering to the graphite surface and to be accommodated there; hence, the number of ions confined between the tip and substrate significantly increases (see Table 1). Here, the ions located below the circular area of radius 1nm with a center at the tip apex are considered as confined ones. Notably, in the case of strong interaction with the substrate, there are cations (anions) not only in the vicinity of the tip but also directly at the positively (negatively) charged surface. The most significant difference in the structure of the confined IL for two strengths of the ion-substrate interaction was found for uncharged and slightly charged surfaces. Figures 3b and e show that for $\varepsilon_{is} = 0.23$ kJ/mol the confined cations are in the flat orientation with all three beads C1, C2 and C3 lying in nearly the same plane, whereas for $\varepsilon_{is} = 70$ kJ/mol the flat and tilted configurations of cations are almost equally populated. This effect is explained by the fact that as the cation-substrate interaction increases, more cations would benefit energetically from adhering to the surfaces and to be accommodated there; hence, they change the orientation to a tilted one. The presence of tilted cations has a profound impact on the friction, because their interactions with the tip increase the sliding energy barriers, which should be overcome during the tip motion.

Table 1. Time averaged surface density of cations and anions confined between the tip and the substrate, which were calculated for three values of surface charge density and two strengths of ion-substrate interaction.

q_s (μC/cm^2)		-32	0	+32
Surface density of cations, N_{cat}/nm^2	$\varepsilon_{is} = 0.23$ kJ/mol	1.9±0.3	0.9±0.1	0.6±0.1
	$\varepsilon_{is} = 70$ kJ/mol	2.5±0.4	1.9±0.3	0.9±0.1
Surface density of anions, N_{an}/nm^2	$\varepsilon_{is} = 0.23$ kJ/mol	0.6±0.1	1.6±0.3	4.4±0.5
	$\varepsilon_{is} = 70$ kJ/mol	1.6±0.3	3.8±0.5	5.4±0.5

To further characterize the effect of charging on the orientation of cations confined between the tip and electrode, we show in Figures 4b-d the dependence of the time averaged fraction of tilted cations on the surface charge density, and the time averaged cation orientation as a function of the lateral distance of the cations from the tip apex. As in the case of the number densities in Figure 3, the cation orientations calculated during sliding are similar to those in equilibrium. The results of simulations show that the charge dependence of the cation orientation is strongly influenced by the strength of the ion-substrate interaction. For the weak interaction, the confined cations on the uncharged surface are mainly in the flat orientation, whereas on the negatively charged surface both tilted and flat oriented cations are represented. In the case of strong interaction, due to a higher concentration of adsorbed cations, we found on average about half the cations in the tilted configuration on both uncharged and negatively charged surfaces. The cation-tip interaction pushes the cation to turn into the flat orientation, and as a result the orientation of the cations located below the tip may differ from the orientation on the rest of the substrate surface (see Figures 4c and d). The tip-induced reorientation of cations provides an additional channel for energy dissipation

in FFM experiments, which may influence the effect of substrate charge on the friction.[43]

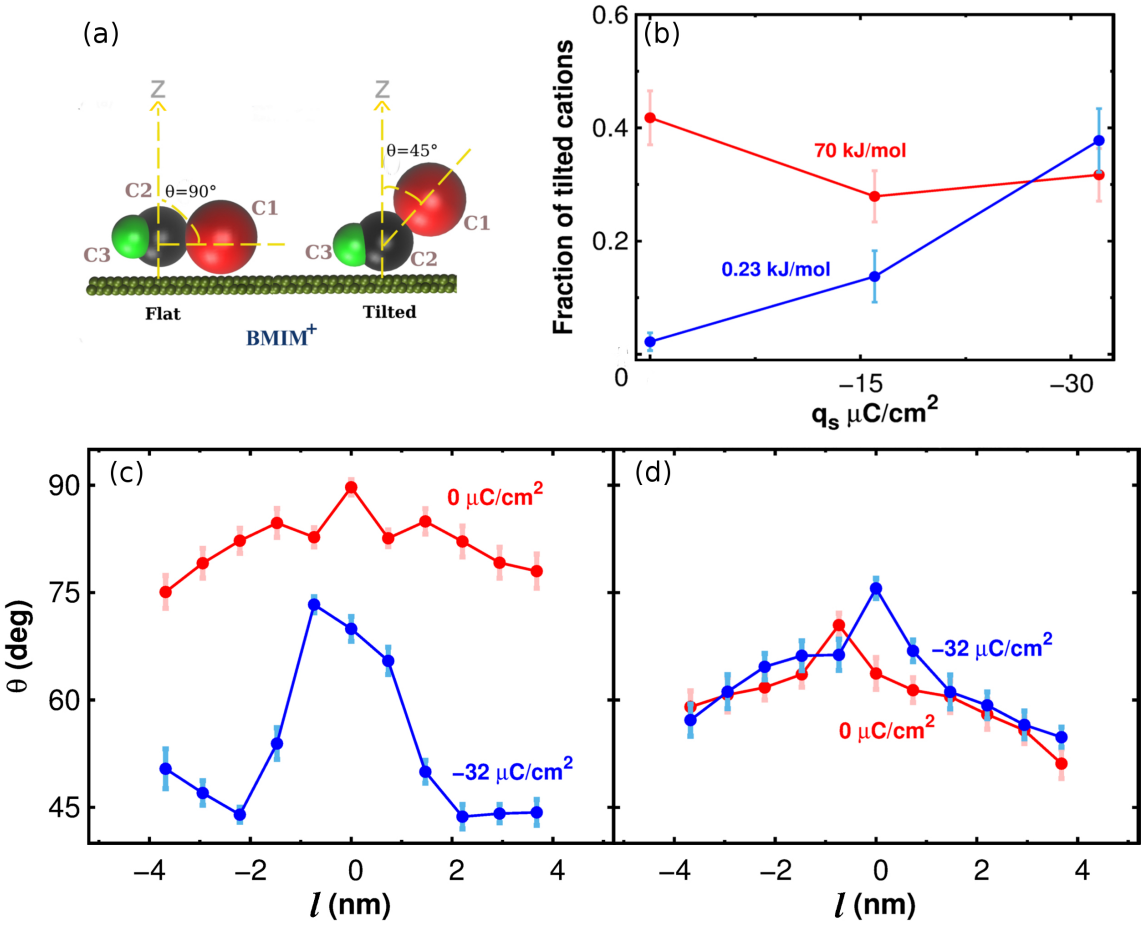


Figure 4. Orientations of cations in the interfacial layer characterized by the angle, θ, between the cation C1-C2 axis and the surface normal. (a) Sketch of the two preferential orientations: 'flat' where $\theta = 90^{\circ}$ and 'tilted' where $\theta = 45^{\circ}$. (b) Dependence of the time averaged fraction of tilted cations in the region confined between the substrate and the tip apex on the substrate surface charge density, shown for the two ion-substrate interactions, ε_{is}. (c)-(d) The time averaged angle, θ, in the interfacial layer as a function of the distance of cations from the tip apex, l, calculated for two values of ion-substrate interaction: (c) $\varepsilon_{is} = 0.23$ kJ/mol, and (d) $\varepsilon_{is} = 70$ kJ/mol. The results are shown for substrate surface charges of 0 and -32 μC/cm^2.

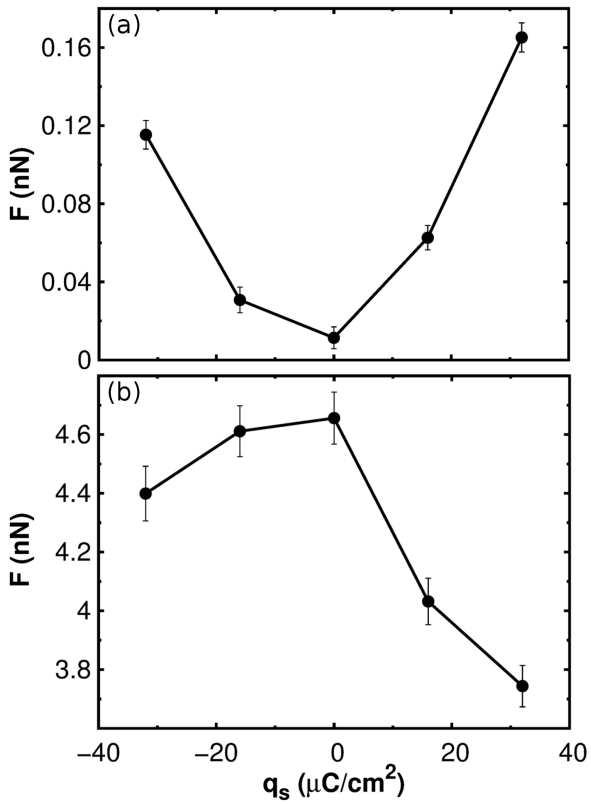


Figure 5. Friction force as a function of substrate surface charge density calculated for two ion-substrate interactions: (a) $\varepsilon_{is} = 0.23$ kJ/mol, where slippage occurs at the interface between the ionic liquid layer and the substrate, and (b) $\varepsilon_{is} = 70$ kJ/mol, where slippage takes place mainly at the interface between the tip and the ionic liquid layer. Here, the simulations are performed for the uncharged tip. Similar results obtained for a negatively charged tip are presented in SI.

The effect of electrode charging on the composition and structure of the confined IL layer leads to a considerable variation of friction force with the substrate surface charge density, $F(q_s)$. The results of simulations presented in Figure 5 show that $F(q_s)$ is highly dependent on the strength of the ion-substrate interaction. For the weak ion-substrate interaction, $\varepsilon_{is} = 0.23$ kJ/mol (see upper panel in Figure 5) the friction force as a function of q_s has a minimum for the uncharged surface and increases by an order of magnitude with the substrate charging of either sign. This can be explained as follows. Due to very low sliding potential energy barriers for ions on such surface (see

Figure 2a), the ions, driven by the tip, slide relatively easily along the substrate, being attached stronger to the tip. Then the frictional energy dissipation mainly occurs at the IL-graphite interface, and its magnitude is proportional to the squared height of the sliding potential energy barriers.[44] With charging of the graphite electrode the distance between the ions and the surface reduces, the ions get deeper into the minima of the surface corrugated landscape, and the barrier heights opposing sliding increase resulting in the enhancement of energy dissipation. This leads to roughly a parabolic growth in the friction force with an increase of surface charge density. The asymmetry of the friction force as a function of the surface charge density with respect to $q_s = 0$ is due to the difference in the heights of potential barriers that oppose the sliding of cation and anion along the substrate surface.

The charge dependence of the friction force correlates well with the variation of the 2D lateral diffusion coefficient calculated for the ions confined between the tip and substrate in equilibrium. The latter has been calculated considering the time evolution of the mean squared displacement of ions located between the fixed tip and substrate and performing averaging over the ensemble of confined ions. The diffusion coefficients of $\sim 1.5 \cdot 10^{-12}$ cm^2/s and $\sim 1.5 \cdot 10^{-13}$ cm^2/s have been obtained for $q_s = 0$ and $|q_s| = 32\ \mu C/cm^2$, respectively. Note, that the diffusion coefficient of the confined layer is significantly lower, ~ 2 orders of magnitude, than that of the ions in bulk at 450 K. The enhancement of ion diffusion results from both the reduction of sliding potential energy barriers at the IL-graphite interface and weakening of the ion-tip interaction, which occur for $q_s = 0\ \mu C/cm^2$. The latter effect is due to the increase of separation between the tip and ions located below it, which was found for low surface charge density (see Figure 3b).

For the strong ion-substrate interaction, $\varepsilon_{is} = 70$ kJ/mol (see Figure 5b), the picture changes drastically. Here, the frictional force has a maximum for the uncharged electrode surface and decreases with increasing charge of any sign. Unlike the case of weak ion-substrate interaction, here the change in the friction force with the density of the surface charge is only 20%. In this case the sliding potential energy barriers at the graphite surface are two orders of magnitude higher than for $\varepsilon_{is} = 0.23$ kJ/mol (see Figure 2), and the coupling between the ions and substrate becomes similar or even stronger than the ion-tip coupling. This affects the regime of motion of ions confined between the tip and substrate. For negatively charged and uncharged graphite electrodes, the time-averaged velocity of the ions is about half the pulling velocity, whereas for the positively charged graphite the anions, which dominate the layer composition, mostly stick to the electrode surface, and the slippage occurs at the IL-tip interface. Unlike the case of the weak ion-substrate interaction, where the frictional energy dissipation occurs at the IL-graphite interface, here it mainly takes place at the IL-tip interface. The observed decrease of friction with increasing $|q_s|$ is explained by a reduction of commensurability between the lateral structure of confined IL layer and the tip lattice, which occurs with the electrode charging (see Suplementary Information). This effect leads to the reduction of sliding potential energy barriers at the IL-tip interface and to the corresponding decrease in the friction force. Since the regime of motion of confined ions depends on the sign of surface charge, the friction as a function of q_s is strongly asymmetric with respect to the zero charge.

To simulate the effect of surface polarization, we have considered a model substrate surface with a fixed charge on it. (Had it been the electronic conductor, we – the main censors- would still have 'allowed' ourselves to try this as a first approximation, although constant potential simulations[45,46] would have been more

accurate in that case). Still the reader may be interested, which scale of potential drops between our charge surface and the bulk of ionic liquids we are here dealing with. This could be calculated for each value of charge in the simulations. We will give here, however, an estimate. The double layer capacitance in such kind of models of ionic liquids is of the order of 10 $\mu F/cm^2$, and thus for the largest charges of $\pm 30\ \mu C/cm^2$ we may roughly speak about ± 3 V, which is a realistic range of polarizations sustainable by many ionic liquid/substrate interfaces.[16,17]

Of course, if the charge of the surface comes out from ionization of surface groups, like it is in the case of mica surfaces, we may start discussing which factors would control this charge, as understanding the effect of pH on the surface charge in the aqueous solution cannot be 'mechanically' translated into the ionic liquid environment. Going in details of chemical reality would be beyond the reach of the considered model. We therefore used the latter as a means of revealing potentially important and, hopefully, generic physical effects.

Conclusions.

In this paper we investigated mechanisms of electrotunable friction studied in FFM experiments with ionic liquids, where only one IL layer is present between the tip and electrode. We demonstrated that the variation of the friction force with the electrode surface charge density is determined by the regime of motion of the confined IL relative to the electrode and tip. The latter depends on the strengths of the ion-electrode and ion-tip interactions and on the commensurability between the characteristic ion dimensions and lattice spacings of the electrode and tip surfaces. Our simulations predicted two strictly different scenarios for the variation of the friction force with the electrode surface charge.

In the first case the ions pulled by the tip mostly slide over the electrode surface, and the slippage plane, where most of energy dissipation occurs, is located at the electrode-IL interface. Then, the friction force as a function of surface charge exhibits a minimum for the zero surface charge, and almost quadratically increases with the charge of any sign. It should be noted that such roughly a parabolic charge dependence of the friction force has not yet been observed in FFM experiments with ionic liquids. However, a significant increase in the friction force with increasing either a positive or negative potential was observed, for example, for sliding on graphite and gold electrodes in Li(G4) TFSI.[47]

The second predicted scenario arises when the pulled ions slip relative to both the electrode surface and the tip, or mainly relative to the tip. In this case, we found a maximum in the friction force at zero surface charge and the reduction of friction with the electrode charging. Our simulations show that this behavior is due to the effect of charging on commensurability between the structure of confined IL and the periodicity of the tip lattice. The observed decrease of friction with increasing $|q_s|$ is explained by a reduction of commensurability between the tip lattice and the lateral structure of confined IL layer, which occurs with the increase of the surface charge density. The predicted variation of the friction force with the surface charge density agrees qualitatively with that observed in FFM experiments using [HMIm][FAP]-IL to lubricate the silica-graphite interface.[11] However, the experimentally observed reduction of friction with surface charging is even larger than that found in simulations. The magnitude of the charge-induced reduction of friction depends on the strength of ion-electrode and ion-tip interactions, the shape and charge distribution of the ions constituting the IL and the structure and chemical reactivity of the tip. In particular, a greater reduction of friction with electrode charging can be expected for amorphous tips

used in experiments[10,11] than for the crystalline one considered in the simulations. There are following reasons for this. Due to the strong counterion-surface attraction at a charged electrode surface, the IL adjacent to the surface acquires a solid-like structure, which is incommensurate with the amorphous tip surface. This should result in a stronger IL slippage on the surface of the amorphous tip sliding over a charged surface, than that found for the crystalline tip. In contrast, at the uncharged surface, where ion-electrode interactions are significantly weaker, the IL layer have a liquid-like structure, and ions are able to attach to energetically favorable sites at the amorphous tip, thus eliminating the slippage at the IL-tip interface. Therefore, with charging the interface, in the case of an amorphous tip we expect to observe a shift of the slippage plane from the IL-electrode to IL-tip interface. Indeed, slippage along the smaller contact area will meet less frictional resistance. A charging-induced shift of the slippage plane from the electrode-IL interface accompanied by a significant reduction of friction has been found in our previous simulations of friction in ILs confined between two flat plates[24,27].

The coarse-grained modelling used here can provide extensive simulation data at a reasonable computational cost and predict qualitative dependencies of friction on surface charge density by averaging over atomistic level information.[48] However, this approach may average out effects connected to the specific molecular structure of the ions and the geometry and, possibly, chemical reactivity of FFM tips that may influence the local energy barriers associated with the motion of ions confined between the tip and electrode. Although a full quantitative description of electrotunable friction may require fully atomistic molecular dynamics simulations, which are planned in our further research, coarse-grained models have shown to capture the key physical mechanisms underlying electrotunable friction. We have addressed this point in our previous works by increasing systematically the complexity of the models.[24,27,29,30] No

doubt, a comparison between the results of these two approaches, coarse-grained vs. atomistic, will allow to understand what effects can be captured by the coarse-grained approach, and which ones cannot, and therefore, such analysis will help to define the range of applicability of such models for the description of friction with ILs. However, as noted above, we expect that the revealed trends in mechanisms of variation of the friction force with electrical polarization of interactive surfaces would be generic for FFM measurements with ILs, since they rely on the effect of long-range electrostatic forces on the ion dynamics. It has been shown that coarse-grained models capture well these effects.

ASSOCIATED CONTENT

Supporting Information

Results of simulations of friction for a negatively charged tip and analysis of the effect of electrode charging on commensurability between the tip lattice and the structure of underlying ionic layer. The Supporting Information is available free of charge on the ACS Publications website at

AUTHOR INFORMATION

Corresponding Authors

*E-mails: karinapi@mail.tau.ac.il; urbakh@post.tau.ac.il

Notes

The authors declare no competing financial interest.

ACKNOWLEDGEMENT

We acknowledge the award of a Research Grant by The Leverhulme Trust (RPG-2016-223). FB acknowledges the financial support from EPSRC (EP/J003859/1). M.U. acknowledges financial the support of the Deutsche Forschungsgemeinschaft (DFG), Grant No. BA 1008/21-1 and COST Action MP1303. O.Y.F. acknowledges support of COST Action MP1303. K.P would like to acknowledge Dr. Davide Mandelli for the useful advices and discussions.

REFERENCES

(1) Urbakh, M.; Klafter, J.; Gourdon, D.; Israelachvili, J. The nonlinear nature of friction. *Nature* **2004**, *430*, 525-528.

(2) Vanossi, A.; Manini, N.; Urbakh, M.; Zaperri, S.; Tosatti, E. Modeling friction: from nanoscale to mesoscale. *Rev. Mod. Phys.* **2013**, *85*, 529-551.

(3) Rozman, M. G.; Urbakh, M.; Klafter, J. Controlling chaotic frictional forces. *Phys. Rev. E* **1998***, 57*, 7340-7343.

(4) Park, J. Y.; Ogletree, D. F.; Thiel, P. A.; Salmeron, M. Electronic control of friction in silicon pn junctions. *Science* **2006**, *313*, 186.

(5) Socoliuc, A.; Gnecco, E.; Maier, S.; Pfeiffer, O.; Baratoff, A.; Bennewitz, R.; Meyer, E. Atomic-scale control of friction by actuation of nanometer-sized contacts. *Science* **2006**, *313*, 207-210.

(6) Lantz, M. A.; Wiesmann, D.; Gotsmann, B. Dynamic superlubricity and the elimination of wear on the nanoscale. *Nat. Nanotechnol.* **2009**, *4*, 586-591.

(7) Drummond, C. Electric-field-induced friction reduction and control. *Phys. Rev. Lett*. **2012**, *109*, 154302.

(8) Nielinger, M.; Baltruschat, H. Nanotribology under electrochemical conditions: influence of a copper (sub)monolayer deposited on single crystal electrodes on friction forces studied with atomic force microscopy. *Phys. Chem. Chem. Phys.* **2007**, *9*, 3965-3969.

(9) Hausen, F.; Gosvami, N. N.; Bennewitz, R. Anion adsorption and atomic friction on Au(111). *Electrochim. Acta* **2011**, *56*, 10694-10700.

(10) Sweeney, J.; Hausen, F.; Hayes, R.; Webber, G. B.; Endres, F.; Rutland, M. W.; Bennewitz, R.; Atkin, R. Control of nanoscale friction on gold in an ionic liquid by a potential dependent ionic lubricant layer. *Phys. Rev. Lett.* **2012**, *109*, 155502.

(11) Li, H.; Wood, R. J.; Rutland, M. W.; Atkin, R. An ionic liquid lubricant enables superlubricity to be ‘‘switched on’’ in situ using an electrical potential. *Chem. Commun.* **2014**, *50*, 4368-4370.

(12) Britton, J.; Cousens, N. E. A.; Coles, S. W.; van Engers, C. D; Babenko, V.; Murdock, A. T.; Koós, A.; Perkin, S.; Grobert, N. A graphene surface force balance. *Langmuir* **2014**, *30*, 11485-11492.

(13) Tivony, R.; Yaakov, D. B.; Silbert, G.; Klein, J. Direct observation of confinement-induced charge inversion at a metal surface. *Langmuir* **2015**, *31*, 12845-12849.

(14) Palacio, M.; Bhushan, B. A review of ionic liquids for green molecular lubrication in nanotechnology. *Tribol. Lett.* **2010**, *40*, 247-268.

(15) Hallett, J. P.; Welton, T. Room-temperature ionic liquids. Solvents for synthesis and catalysis. *Chem. Rev.* **2011**, *111*, 3508-3576.

(16) Fedorov, M.; Kornyshev, A. Ionic liquids at electrified interfaces. *Chem. Rev.* **2014**, *114*, 2978-3036.

(17) Hayes, R.; Warr, G. G.; Atkin, R. Structure and nanostructure in ionic liquids. *Chem. Rev.* **2015**, *115*, 6357-6426.

(18) Bazant, M. Z.; Storey, B. D.; Kornyshev, A. A. Double layer in ionic liquids: overscreening versus crowding. *Phys. Rev. Lett.* **2011**, *106*, 046102.

(19) Smith, A. M.; Lovelock, K. R. J.; Gosvami, N. N.; Welton, T.; Perkin, S. Quantized friction across ionic liquid thin films. *Phys. Chem. Chem. Phys.* **2013**, *15*, 15317-15320.

(20) Comtet, J.; Nigués, A.; Kaiser, V.; Coasne, B.; Bocquet, L.; Siria, A. Nanoscale capillary freezing of ionic liquids confined between metallic interfaces and the role of electronic screening. *Nat. Mater.* **2017**, *16*, 634-639.

(21) Mendoca, A. C. F.; Pauda, A. A. H.; Malfreyt, P. Nonequilibrium molecular simulations of new ionic lubricants at metallic surfaces: prediction of the friction. *J. Chem. Theory Comput.* **2013**, *9*, 1600-1610.

(22) Mendoca, A. C. F.; Fomin, Y. D.; Malfreyt, P.; Pauda, A. A. H. Novel ionic lubricants for amorphous carbon surfaces: molecular modeling of the structure and friction. Soft Matter **2013**, *9*, 10606-10616.

(23) Canova, F. F.; Matsubara, H.; Mizukami, M.; Kurihara, K.; Shluger, A. L. Shear dynamics of nanoconfined ionic liquids. *Phys. Chem. Chem. Phys.* **2014**, *16*, 8247-8256.

(24) Fajardo, O. Y.; Bresme, F.; Kornyshev, A. A.; Urbakh, M. Electrotunable lubricity with ionic liquids nanoscale films. *Scientific Reports* **2015**, *5*, 7698.

(25) Capozza, R.; Vanossi, A.; Benassi, A.; Tosatti, E. Squeezout phenomena and boundary layer formation of a model ionic liquid under confinement and charging. *J. Chem. Phys.* **2015**, *142*, 064707.

(26) Capozza, R.; Vanossi, A.; Benassi, A.; Tosatti, E. Electrical charging effects on the sliding friction of a model nano-confined ionic liquid. *J. Chem. Phys.* **2015**, *143*, 144703.

(27) Fajardo, O. Y.; Bresme, F.; Kornyshev, A. A.; Urbakh, M. Electrotunable friction with ionic liquid lubricants: how important is the molecular structure of the ions? *J. Phys. Chem. Lett.* **2015,** *6*, 3998-4004.

(28) Voeltzel, N.; Gulliani, A.; Vergne, P.; Fillot, N.; Joly, L. Nanolubrication by ionic liquids: molecular dynamics simulations reveal an anomalous effective rheology. *Phys. Chem. Chem. Phys.* **2015**, *35*, 23226-23235.

(29) Fajardo, O. Y.; Bresme, F.; Kornyshev, A. A.; Urbakh, M. Water in ionic liquid lubricants: friend and foe. *ACS Nano* **2017**, *11*, 6825-6831.

(30) David, A.; Fajardo, O. Y.; Kornyshev, A. A.; Urbakh, M.; Bresme, F. Electrotunable lubricity with ionic liquids: the influence of nanoscale roughness. *Faraday Discuss.* **2017**, *199*, 279-297.

(31) Roy, D.; Maroncelli, M. An improved four-site ionic liquid model. *J. Phys. Chem. B* **2010**, *114*, 12629-12631.

(32) Li, H.; Rutland, M. W.; Atkin, R. Ionic liquid lubrication: influence of ion structure, surface potential and sliding velocity. *Phys. Chem. Chem. Phys.* **2013**, *15*, 14616-14623.

(33) Werzer, O.; Cranston, E. D.; Warr, G. G.; Atkin, R.; Rutland, M. W. Ionic liquid nanotribology: mica-silica interactions in ethylammonium nitrate. *Phys. Chem. Chem. Phys.* **2012**, *14*, 5147-5152.

(34) Atkin, R.; Warr, G. G. Structure in confined room-temperature ionic liquids. *J. Phys. Chem. C* **2007**, *111*, 5162-5168.

(35) Shimizu, K.; Pensado, A.; Malfreyt, P.; Pádua, A. A. H.; Canongia Lopes J. N. 2D or not 2D: Structural and charge ordering at the solid-liquid interface of the 1-(2-hydroxyethyl)-3-methylimidazolium tetrafluoroborate ionic liquid. *Faraday Discuss.* **2012**, *154*, 155-169.

(36) Merlet, C.; Salanne, M.; Rotenberg, B.; Madden, P. A. Imidazolium ionic liquid interfaces with vapor and graphite: interfacial tension and capacitance from coarse-grained molecular simulations. *J. Phys. Chem. C* **2011**, *115*, 16613-16618.

(37) Gao, J. P.; Luedtke W. D.; Landman, U. Structure and solvation forces in confined films: linear and branched alkanes. *J. Chem. Phys*. **1997**, *106*, 4309-4318.

(38) Gao, J.; Luedtke W. D.; Lamndan, U. Friction control in thin-film lubrication. *J. Phys. Chem. B* **1998**, *102*, 5033-5037.

(39) Camara, L. G.; Bresme, F. Molecular dynamics simulations of crystallization under confinement at triple point conditions. *J. Chem. Phys.* **2003**, *119*, 2792-2800.

(40) Sugimoto, Y.; Yurtsever, A.; Abe, M.; Morita, S.; Ondráček, M.; Pou, P.; Pérez, R.; Jelínek, P. Role of tip chemical reactivity on atom manipulation process in dynamic force microscopy. *ACS Nano* **2013**, *7*, 7370-7376.

(41) Bussi, G.; Donadio, D.; Parrinello, M. Canonical sampling through velocity rescaling. *J. Chem. Phys.* **2007**, *126*, 014101.

(42) Berendsen, H. J. C.; van der Spoel, D.; van Drunen, R. Gromacs – a message passing parallel molecular-dynamics implementation. *Comput. Phys. Commun*. **1995**, *91*, 43-56.

(43) de Wijn, A. S.; Fasolino, A.; Filippov, A. E.; Urbakh, M. Nanoscopic friction under electrochemical control. *Phys. Rev. Lett*. **2014**, *112*, 055502.

(44) Cieplak, M.; Smith, E. D.; Robbins, M. O. Molecular-origins of friction - the force on adsorbed layers, *Science* **1994**, *265*, 1209-1212.

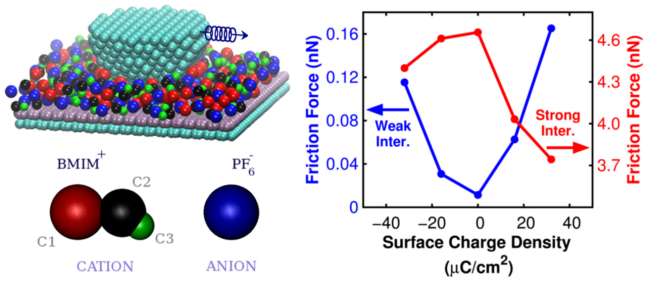
(45) Merlet, C.; Rotenberg, B.; Madden, P. A.; Salanne, M. Computer simulations in ionic liquids at electrochemical interfaces. *Phys. Chem. Chem. Phys*. **2013**, *15*, 15781-15792.

(46) Kondrat, S.; Wu, P.; Qiao, R.; Kornyshev, A. A. Accelerating charging dynamics in subnanometre pores. *Nat. Mater*. **2014,** *13*, 387-393.

(47) Li, H.; Rutland, M. W.; Watanabe, M.; Atkin, R. Boundary layer friction of solvate ionic liquids as a function of potential. *Faraday Discuss.* **2017**, *199*, 311-322.

(48) Wang, Y.; Izvekov, S.; Yan, T.; Voth, G. A. Multiscale coarse-graining of ionic liquids. *J. Phys. Chem. B* **2006**, *110*, 3564-3575.

TOC Graphic.


BMIM+
PF6-
C2
C1
C3
CATION
ANION
Friction Force (nN)
0.16
0.12
0.08
0.04
0
Weak Inter.
Strong Inter.
4.6
4.3
4.0
3.7
Friction Force (nN)
−40
−20
0
20
40
Surface Charge Density
(μC/cm2)